

The zebrafish as *MYCN* amplified *nipbl* deactivated neuroblastoma model

1. Sort description of research agenda & general goals :

Neuroblastoma is a malignant tumor of the peripheral nervous system most commonly arising in children under the age of 2. With half of all patients sharing a 5 year survival rate lower than 50% the importance of identifying novel genes implicated in its development is evident. The most important prognostic factor for neuroblastoma is the *MYCN* amplification status. A *MYCN* amplification is found in about 20% of cases and is often associated with especially poor disease development. Recent studies show that *NIPBL*, a cohesin loading factor, is often deactivated in neuroblastoma patients, suggesting cooperation with known tumor driving genes like *MYCN*. The cohesin ring is an essential protein complex for DNA repair, sister chromatid cohesion and most notably gene expression during the cell interphase. In the interphase cohesin forms chromatin loops and creates regions of high and low gene transcription. Even though a dysregulation of one of the cohesin complex genes is associated with a multitude of different tumor types, the targets and effects of such a dysregulation remain poorly understood making further research imperative.

To investigate further in the role of *NIPBL* in neuroblastoma we used a CRISPR/Cas 9 system to establish a *nipbl* haploinsufficient, *MYCN* amplified zebrafish neuroblastoma model. This model will enable the study of *NIPBL*'s effect on tumor initiation and development.

2. Detailed description of research problem :

2.1 An introduction to Neuroblastoma

Neuroblastoma is the most common noncranial solid tumor found in children and accounts for approximately 10% of all pediatric cancer-related deaths (1). Neuroblastoma arises from the sympathoadrenal lineage of the neural crest most likely due to a deregulation of pro proliferative and pro differentiation factors during neural crest development (2). 90% of neuroblastomas are diagnosed in children under the age of 5. They are most commonly found in the abdomen where they are often associated with the adrenal gland or sympathetic ganglia (3–5). Neuroblastoma shows great genetic and biological heterogeneity, with multiple mutations being necessary for the formation of fully malignant tumor cells (4,6–8). The prognosis for neuroblastoma patients also widely differs from case to case with low and immediate risk patients having a survival rate close to 100% and high risk patients having a 5 year survival rate of less than 50% (4,8–11). Low risk and intermediate risk patients often show tumors that can be treated by moderate doses of chemotherapy, surgical removal or observation alone (12,13), whereas high risk patients display tumors that show low to no response to intensive chemotherapeutic treatment and often metastasize to the bone marrow and lymph nodes (14,15). With 50% of neuroblastoma patients being classified as high risk (15), it is of imperative that novel therapeutic targets and genes playing a role in neuroblastoma tumorigenesis are investigated into.

2.2 *MYCN* status as hallmark of poor prognosis neuroblastoma

Although age, stage of the disease and tumor differentiation are important prognostic factors of neuroblastoma, the most important prognostic factor for a poor prognosis is the *MYCN* amplification status (15,16). A *MYCN* amplification is found in about 20% of patients and in about 50% of all poor prognosis neuroblastomas (16,17). The *MYCN* amplification is always present at diagnosis and is never acquired during later stages of the disease. This suggest that a

MYCN amplification is an early or initiating event however, not much is known about when and how the amplification is acquired. (18)

MYCN belongs to the family of *MYC* genes and is closely related to the *C-MYC* and *L-MYC* genes. *MYC* proteins are transcription factors which bind to active promoters and enhancer to regulate the expression of over 15% of all genes in a cell (18). Hence, the *MYC* proteins are master regulators of cell fate and play a crucial role in cell-differentiation, proliferation, senescence, growth, metabolism and apoptosis (19). Deregulation of *MYC* is often associated with a whole array of pediatric and adult cancers. It is believed that a dysregulation of *MYC* can be found in around 70% of human cancers (20). A study conducted by The Cancer Genome Atlas (TCGA) investigating mutations across 33 tumor types and 9000 samples showed that 28% of human cancers have an amplification of at least one of the *MYC* genes (21). *C-MYC* amplifications are found frequently in ovarian cancer (64%), esophageal cancer (45.3%) squamous lung cancer (37.2%) and breast cancer (30%) (20). In most cancer an amplification of one of the *MYC* genes is associated with the worst possible prognosis. *L-* and *N-MYC* are rarely amplified in tumors (7%) but *N-MYC* amplification can be found in tumors possessing neuroendocrine features.

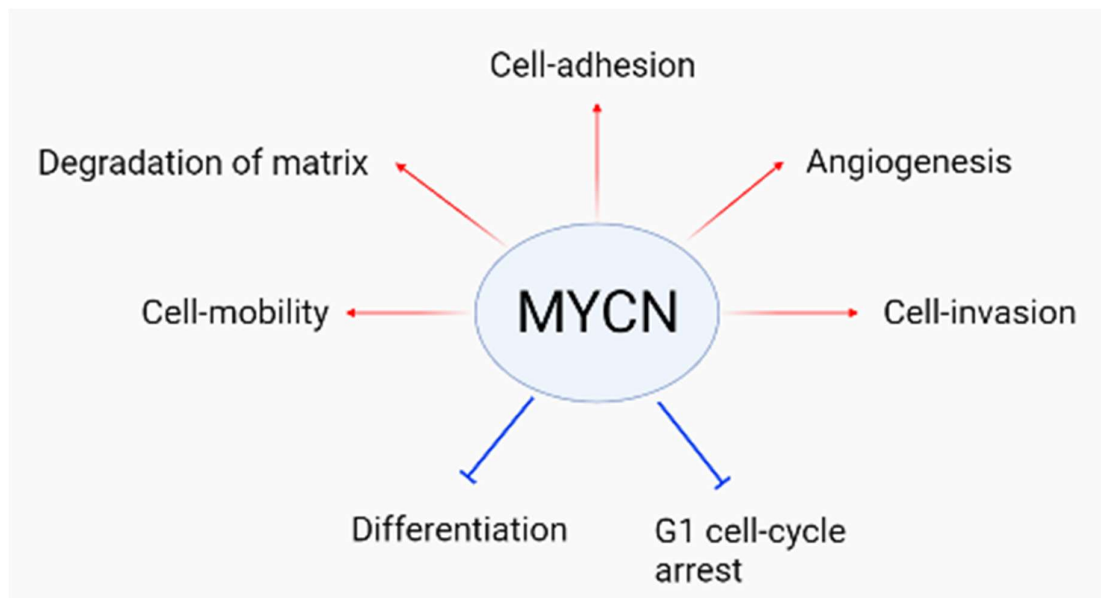


Figure 1: *MYCN* overexpression strongly promotes tumor growth and migration. *MYCN* amplified neuroblastoma tumors are high risk. *MYC* genes are dysregulated in 70% of human tumors.

In contrast to *C-MYC*, *MYCN* expression is tissue specific and found only during early developmental stages (22). Overexpression of *MYCN* drives neuroblastoma tumorigenesis in many ways. When overexpressed, *MYCN* promotes tumor metastasis in many ways by acting on cell-adhesion, mobility, invasion and the degradation of surrounding matrices (22). *MYCN* overexpression correlates with high vascularity and poor prognosis suggesting that *MYCN* drives angiogenesis further augmenting the chance of dissemination (23–25). *MYCN* promotes self-renewal and a stem-like state by blocking pro differentiation pathways and upregulating the expression of self-renewal and pluripotency factors (26–30). *MYCN* overexpression also promotes cell proliferation and cell cycle progression. *MYCN* driven cancer cells show an inability to enter G1 cell cycle arrest due to DNA damage. However *MYCN* also promotes apoptosis and partially slows down the cancers progression (22).

2.3 *MYCN* does not act alone

Another important prognostic factor is the *Anaplastic Lymphoma Kinase* or *ALK* gene status. An *ALK* gene amplification is found in about 15% of all *MYCN* amplified neuroblastomas (31,32) and an *ALK* mutation is the most common mutation in familial neuroblastoma. The identification of *ALK* as an important prognostic factor and therapeutic target, underlines the genetic heterogeneity of neuroblastoma and the importance of identifying more genes playing a role in poor prognosis neuroblastoma. Patients with amplified *MYCN* and *ALK* share a particularly poor prognosis(31–34). Using the zebrafish as model, it was discovered that *alk* blocks the apoptotic death of *MYCN* overexpressing neuroblasts and therefore acts in concert with *MYCN* to drive tumorigenesis (7). Fish co-expressing activated *alk* and human *MYCN* developed tumors with accelerated tumor onset and almost tripled tumor penetrance (5,7,35).

We believe that *nipbl* act as a tumor suppressor gene for neuroblastoma. A deactivation of one copy of *nipbl* may enhance the effects of an *MYCN* amplification.

2.4 *Nipbl* is often deactivated in childhood cancers

Recent findings emerging from pediatric cancer studies at St Jude show that many primary childhood cancers at diagnosis have undergone selection for mutations affecting the *NIPBL* genes, which normally work together to establish the 3D architecture of the nucleome (36). *NIPBL* is known to act as a cohesion loading factor, allowing the binding of the cohesin protein complex to chromatin. The proteins encoded by *NIPBL* and other cohesin related genes act in concert to establish insulated neighborhoods that restrict the actions of powerful enhancers and repressors to the genes they are intended to regulate. As recurring mutations of cohesin genes were detected in multiple types of childhood cancers, it is imperative to investigate the mechanisms controlling this aspect of the initiation and maintenance of these neoplasms(36–40). To address this issue we propose to establish a zebrafish neuroblastoma model in which we can study the role of *nipbl* deactivation on tumorigenesis.

2.5 3D structure of our genome

To fit the 46 chromosomes of the human genome, they have to be compacted and organized inside the nucleus. Each chromosome has a distinct position within the nucleus called chromosome territory. Gene rich chromosomes are generally located close to the center of the nucleus, whereas gene poor chromosomes can be found on the periphery of the nucleus(41,42). These territories can be further divided into chromosomal A&B compartments. The A compartment contains gene rich regions of the chromosome and similarly to the chromosome territories tends to be placed close to the center of the nucleus. Compartment B contains gene poor regions and tends to be placed on the periphery of the nucleus(41,42).

The next level of organization involves topologically associating domains also known as TADs. TADs are DNA sequences up to 2 Mb in size that physically interact more frequently with themselves than other sequences. These sequences therefore form insulated neighborhoods within the nucleus that control the access of transcriptional activators and inhibitors to their target gene. The recurring theme of gene rich regions being placed in the center and gene poor regions being

placed at the periphery of the TAD can also be found here. The TADs themselves are composed by chromatin loops formed by the cohesin ring complex(42). The formation of TADs and organization of DNA inside the nucleus has found to be cell type specific but little is know about the mechanism underlying the cell type specific organization of DNA in human.

2.6 The cohesin ring complex: a key regulator of the genome

The non-random organization of chromatin into territories, compartments, TADs and loops causes physical contacts between target genes and the respective enhancers which directly stands in correlation with transcriptional control and gene regulation(43,44). The formation of TADS and therefore gene transcription are tightly regulated by the cohesin complex and it loading proteins. To form TADs from chromatin, human cells use a protein complex named the cohesin ring. Cohesin is a ubiquitously expressed multi-protein complex that has a central role in the nuclear organization of eukaryotes. The complex forms a ring that can encircles two strands of chromatin to regulate sister chromatid cohesion (SCC), as well as the maintenance of chromatin looping structure, transcription and DNA repair(45–48). For a long time research had been focused on cohesins role in SCC even though most cellular cohesin functions in interphase (49). In the interphase the cohesin ring entraps 2 chromatin fibers and forms loops by extruding the one chromatin fiber past the other. It is suggested that during this process transcription factors attach to the cohesin ring until the complex extrudes the transcription factors target sequence. When this happens the transcription factor detaches from cohesin and binds to its sequence. The extruding of DNA stops once cohesin encounters a CTCF site that through forming a homologue with another CTCF site blocks the rings extrusion. The loops created by cohesin frequently correspond to TADs that form regions of gene transcription within the nucleus(42,50). Recent studies have shown that cellular regions that are depleted of cohesin are enriched in pluripotency genes (51) further implicating *nipbl* in the domain of gene regulation.

The zebrafish as *MYCN* amplified *nipbl* deactivated neuroblastoma model. Sexl M.

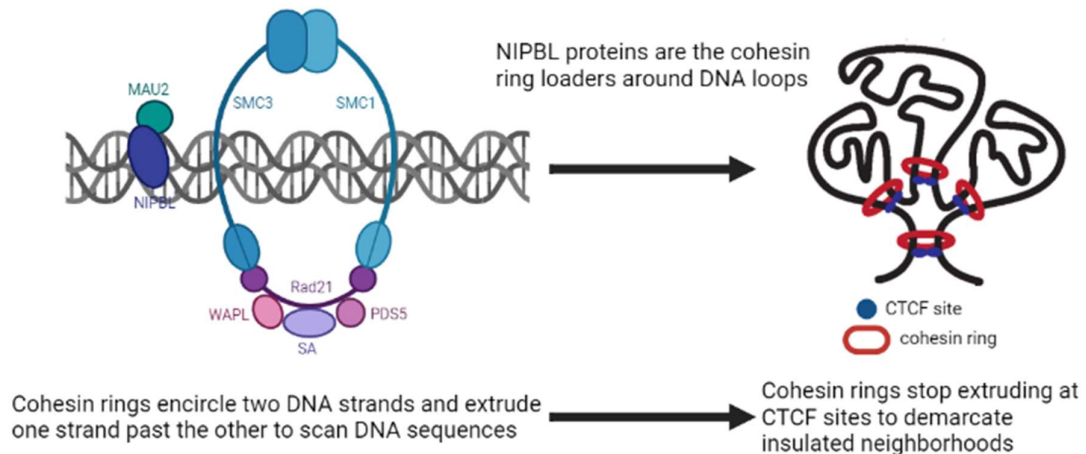


Figure 2: Cohesin forms chromatin loops and acts on gene expression.

2.7 Animal models of neuroblastoma

Most studies of neuroblastoma use immortalized tumor cells derived from patient samples. Even though *in vitro* studies are able to give great insight into tumor development and maintenance of neuroblastoma, they are limited by the lack of physiological complexity of the normal tumor environment (35). As the development of neuroblastoma starts with embryogenesis and the migration of neural crest cells through various tissue types, cancer cells are exposed to a multitude of extracellular signaling molecules stemming from cells of multiple lineages in the microenvironment. It's very hard to study such complex cell-cell interactions *in vitro*. Furthermore, the essential molecular and cellular events involved in tumor initiation cannot be studied using transformed tumor cells *in vitro*. The limitation of *in vitro* systems underlines the importance of *in vivo* models for neuroblastoma.

When selecting an animal neuroblastoma model several important questions arise: Is the animal physiologically and genetically comparable to humans? Do tumors develop in a reasonable amount of time? Are the developed tumors similar in location, histology and immunohistochemistry? Can tumor development and progression be conveniently monitored without having to sacrifice the animal? Are techniques for gene editing readily available? Can the animal model reproduce

quickly and in high numbers? Is the animal suitable for large scale drug-screening and pharmacologic studies? (5)

The first in vivo models of neuroblastoma were developed through xenografts of human neuroblastoma cells in immunosuppressed mice (5,17). In the 1990 the first transgenic mouse model for neuroblastoma was developed by overexpressing *MYCN* under the tyrosine hydroxylase promoter (17,52). The models were successful in developing tumors similar to human neuroblastoma but were still limited by small litter size, cost and the inability to conveniently monitor tumor initiation, development and maintenance. To address those issues, Look and colleagues established a zebrafish model complementing the already existing human and rodent models (7). Multiple features of zebrafish make its utilization as a model for neuroblastoma stand out.

2.8 The zebrafish as animal model

Zebrafish possess 26,206 protein coding genes with 71% having human orthologues. 82% of human disease associated genes listed on the “Online Mendelian Inheritance in Man” database can be connected to a zebrafish orthologue, suggesting that the major pathways involved with human disease can also be found in zebrafish(53,54). Successful establishment of the zebrafish as model for diverse types of cancer like leukemia, prostate cancer or skin cancer further supports this suggestion (55–58).

A key advantage of zebrafish as an vertebrate animal model is that zebrafish generate high numbers of offspring in short periods of time. They reach sexual maturity in an average of 12 weeks and can be mated weekly with each female fish laying up to 100 eggs each mating. Additionally, cost and expense of maintaining large populations of fish are considerably lower than with any murine model.

Furthermore, a unique feature of juvenile and pigment deficient mutant adult zebrafish is their translucence, as their organs can easily be visualized by microscopy or with the naked eye. Their translucence combined with tissue

The zebrafish as *MYCN* amplified *nipbl* deactivated neuroblastoma model. SexI M.

specific expression of Enhanced Green Fluorescent Protein (EGFP) allow easy and convenient monitoring of tumor development and growth (see figure 1).

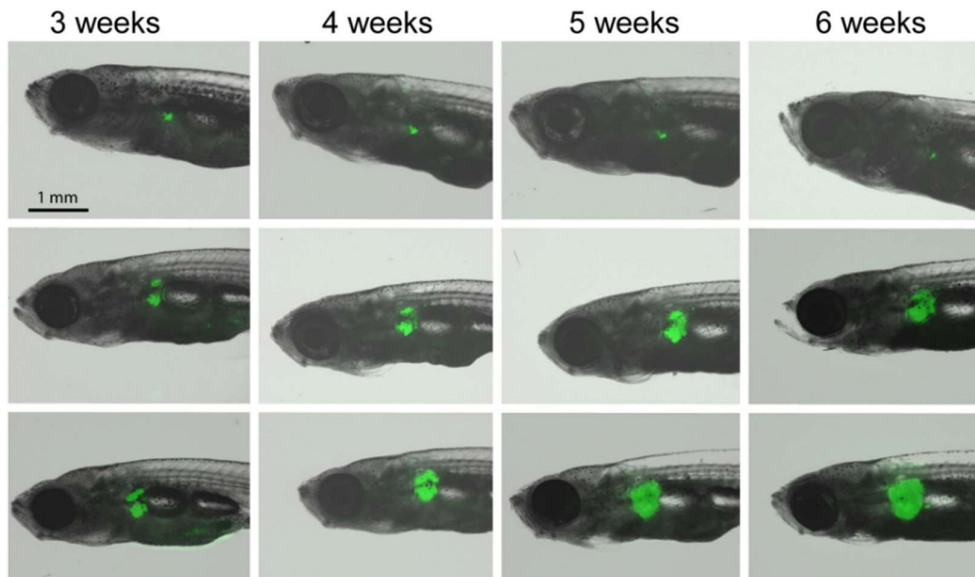


Figure 3: Tumor development of mutant *nf1a* *MYCN*-GFP fish. The tumors can be seen with the naked eye. This figure was adapted from Synergy between loss of *NF1* and overexpression of *MYCN* in neuroblastoma is mediated by the GAP-related domain, Shuning He, 2016, *e-Life*. Adapted with permission.

2.9 Zebrafish models of neuroblastoma

In 2012 the Look lab published the first zebrafish neuroblastoma model (7). They demonstrated that the injection of a transgenic construct of *EGFP* driven by the *dopamine-β-hydroxylase* (*dβh*) promoter (*dβh:EGFP*), resulted in stable transgenic zebrafish expressing EGFP in the sympathetic ganglia and interrenal gland, which is the zebrafish equivalent of the adrenal gland (7). When overexpression of an EGFP-*MYCN* fusion was driven by the same *dβh* promoter (*dβh:EGFP-MYCN*) in zebrafish, *MYCN* was overexpressed in the sympathetic ganglia and interrenal gland. The overexpressed *MYCN* subsequently caused formation of tumors in the interrenal gland. The formed tumors arose 10 to 20 weeks post fertilization and closely resembles human *MYCN* driven neuroblastoma(7). The tumors expression

of EGFP, fused with MYCN, made it possible to monitor its formation and development with the naked eye. In contrast, *dβh:EGFP* fish also expressed EGFP in the sympathetic ganglia and interrenal gland, but both structures are too small to be recognized by the naked eye. The creation of this novel *MYCN* driven neuroblastoma model now allows the identification and study of novel genes implicated in *MYCN* driven neuroblastoma. Furthermore, after breeding the *dβh:EGFP-MYCN* zebrafish with a *dβh:ALK; dβh:EGFP* transgenic zebrafish line, the Look lab was able to demonstrate that a co-overexpression of MYCN and activated ALK resulted in the formation of tumors only 5 to 7 weeks post fertilization. The tumor penetrance was tripled in fish with simultaneous overexpression of ALK and MYCN(7).

2.10 Genome editing with CRISPR/Cas9 systems in zebrafish

In order to study the role of *nipbl* in zebrafish neuroblastoma model, CRISPR/Cas9 technology is applied to generate mutations in zebrafish *nipbl* genes (See figure 3). The discovery of Clustered Regularly Interspaced Short Palindromic Repeat (CRISPR) / Associated Protein (Cas) systems, a form of adaptive immune system in bacteria and archaea, has revolutionized genome editing. Many different CRISPR systems have been identified in bacteria and archaea, however the type II CRISPR/Cas9 system has become irreplaceable for in vivo studies (59). In bacteria this system takes up foreign DNA from phages and integrates it as CRISPR sequence. The bacteria then continues to transcribe the newly integrated sequence and create a short CRISPR RNA or crRNA. After fusion with a transactivating crRNA (tracrRNA), the tracrRNA-crRNA complex can bind to and activate the Cas9 protein. The crRNA acts as template and guides the Cas9 protein to the corresponding genomic sequence where Cas9 generates double strand breaks and removes the targeted sequence effectively getting rid of the phages DNA(60,61). In 2020 Emmanuelle Charpentier and Jennifer Doudna were awarded a noble prize for their work on CRISPR. They replaced the crRNA and tracrRNA with a single RNA molecule called guide RNA (gRNA). Upon binding to Cas9, the gRNA-Cas9 complex binds to the complementary genomic sequence and starts cleaving, generating double strand breaks(62,63). DNA repair

mechanisms are recruited to the site of damage and repair the break, possibly leaving behind deactivating mutations.

In recent years this novel genome editing technology was adapted to many animal models, including the zebrafish(59,64–66). By injecting a guide RNA and the mRNA for Cas9 in unicellular zebrafish embryos, genes can be knocked out with relative ease(34,35). This system was recently further improved by injecting Cas9 protein instead of mRNA.

The proposed project will use the CRISPR/Cas9 system to inactivate *nipbl* by generating frame-shifting mutation in the *nipbl* gene. By crossing the *nipbl* mutants with fish overexpressing *MYCN*, we hope to gain insight on the effects of *nipbl* inactivation in the tumorigenesis of *MYCN* driven neuroblastoma (See Figure 3).

Importantly, the CRISPR/Cas9 system, as an efficient genome editing tool, is also known to generate off target mutations, which are also called scars(68). To rule out their influence on the proposed experiment, knockouts always have to be generated with 2 different gRNA constructs targeting different exons of the same gene. Because different gRNA sequences are likely to cause scars in different regions of the genome, if the mutant fish resulted from injection with one construct show the same phenotype as the fish resulted from injection with the other construct, it would suggest that the phenotype is likely caused by the on-target inactivation of the target gene and not the off-target CRISPR scar.

3. Methodological considerations :

Overview :

Recent studies emerging from the St. Jude Children's Research Hospital show that *NIPBL* and other with cohesin associated genes are often mutated in pediatric cancer patients, including neuroblastoma. The proposed project aims to elucidate the role of *NIPBL* by establishing a *MYCN* driven neuroblastoma zebrafish model with deactivated *nipbl* gene.

We used a CRISPR/Cas9 system to generate the loss-of-function mutations of zebrafish *nipbl* genes. As *nipbl* has been duplicated in zebrafish genome, there are two zebrafish orthologs, *nipbla* and *nipblb*. Both *nipbla* and *nipblb* were knocked out in this project. The 4 alleles of *nipbl* in zebrafish will allow us to not only reduce the gene expression to 50%, but also to 25% and 75%. A complete knockout of one of the cohesin genes (except *STAG2* as it is partially compensated by *STAG1*) is embryonic lethal in eukaryotes. To rule out the influence of off target CRISPR scars on our model, each gene has to be targeted by two different CRISPR gRNA constructs. We therefore used a total of 4 CRISPR gRNA construct: 2 aiming to deactivate *nipbla* and 2 aiming to deactivate *nipblb*.

To generate the first generation of mutants, zebrafish embryos at the unicellular stage were injected with Cas 9 protein and gRNA targeting one of the 2 *nipbl* genes. The CRISPR system then generated double strand DNA breaks when the embryo had 8 to 16 germ cells (resulting in 8 to 16 different *nipbl* genotypes in F1 offspring). The zebrafishes DNA repair mechanism proceed to repair the break and possibly generate a frame shifting mutation. The injected embryos were raised to adulthood for mutation analysis.

We used a combination of Polymerase Chain Reaction (PCR), T-7 endonuclease I assay and sequencing to identify *nipbl* mutations generated by CRISPR/Cas9. After lysis of a small zebrafish tissue sample, genomic DNA was isolated and a PCR was used to amplify a selected genome region of *nipbl* around the CRISPR targeted site. When there is a heterozygous mutation in the region, the T-7

endonuclease I enzyme can recognize the mismatch in the DNA sequence and cut at the site, resulting in smaller DNA fragments that can be easily be detected via gel electrophoresis. DNA from all suspected mutants will then be sent for sequencing so that frame-shifting mutations can be identified. Notably, the T-7 endonuclease I assay cannot be used for screening of homozygous mutants as no DNA mismatch can be detected in a homozygous mutant. The samples of suspected homozygous mutants will need to be sequenced directly.

First, we needed to identify F0 founder zebrafish, in which the germ cells were mutated by CRISPR/Cas. Zebrafish raised from embryos injected with CRISPR/Cas (which is called 'injectant') were bred with wild-type (wt) fish (see figure 2). If a germ cell was mutated, the resulted offspring embryos were heterozygous mutants, which were identified using T-7 endonuclease I. Thus, we collected 16 embryos from each breeding pair and use the combination of PCR and T-7 endonuclease I assay, as described above, to look for embryos containing *nipbl* mutations. If mutations can be identified in the offspring, the corresponding parental injectant zebrafish were identified as a founder (F0).

Next, offspring of the F0 & wt pair were raised to adulthood. These adult were genotyped using genomic DNA extracted from a small piece of the tail fin. Mutant identified through PCR and T-7 endonuclease I assay were sent for sequencing. Sequence from each fish will then be manually analyzed. Previous experience tells us that the CRISPR/Cas system can generate multiple germ line mutations in a F0 fish. We will only keep the fish acquired frameshift mutations as F1 mutants for this project.

Because there are two *nipbl* genes in zebrafish, and we used two gRNA constructs to target each gene, we identified 4 separate population of F1 fish: two heterozygous *nipbla* (*nipbla1* +/- and *nipbla2* +/-) and two heterozygous *nipblb* (*nipblb1* +/- and *nipblb2* +/-).

Once we had identified enough F1 mutants with heterozygous deactivated *nipbl*, they were mated with *MYCN* overexpressing zebrafish (*dβh:EGFP-MYCN; dβh:EGFP*) to obtain F2 generation (see figure 2). This mating step helps to dilute off-target CRISPR scars, and to introduce *MYCN* transgene into *nipbl* mutants for

further neuroblastoma research. We established the same 4 sets of *nipbl* mutant zebrafish in the resulted *MYCN* overexpressing F2 zebrafish: two heterozygous *nipbla* (*nipbla1 +/-* and *nipbla2 +/-*) and two heterozygous *nipblb* (*nipblb1 +/-* and *nipblb2 +/-*). In addition, each F2 set will be divided into two subsets: *MYCN*-positive, and *MYCN*-negative.

Subsequently, we mated heterozygous *nipbla1* F2 mutants with the heterozygous *nipblb1* F2 fish. This mating will result in 2 important F3 populations of fish: *nipbla1+/- ; nipblb1+/-*, and *nipbla2+/- ; nipblb2+/-*. The project has not been completed at the date of this report. The following steps are handled by the Look laboratory:

Both groups of fish will then have one allele of each *nipbl* gene deactivated. To identify the *nipbla* and *nipblb* mutations, we will again use the combination of PCR, T-7 endonuclease I assay and sequencing as described above.

Then, we will perform an in cross of the F3 *nipbla1 +/- ; nipblb1 +/-*; *MYCN*-negative fish, to generate all possible 9 combinations of NIPBL genotypes (see figure 2):

- | | |
|--------------------------------------|--------------------------------------|
| (1) <i>nipbla1 +/- , nipblb1 +/+</i> | (2) <i>nipbla1 -/- , nipblb1 +/+</i> |
| (3) <i>nipbla1 +/+ , nipblb1 +/-</i> | (4) <i>nipbla1 +/+ , nipblb1 -/-</i> |
| (5) <i>nipbla1 +/- , nipblb1 +/-</i> | (6) <i>nipbla1 -/- , nipblb1 +/-</i> |
| (7) <i>nipbla1 +/- , nipblb1 -/-</i> | (8) <i>nipbla1 -/- , nipblb1 -/-</i> |
| (9) <i>nipbla1 +/+ , nipblb1 +/+</i> | |

We will carefully observe the offspring of this breeding, to look for developmental phenotypes and maybe death caused by *nipbl* mutations. We will also perform the same in-cross of the F3 *nipbla2+/- ; nipblb2+/-*; *MYCN*-negative fish, to compare the phenotypes resulted from mutations caused by different gRNA targeting different regions of the same gene. We expect the true effects of loss-of-function mutations of *nipbl*, but not the random off-target effects, will be reproduced in fish with different mutations on the same gene.

The zebrafish as *MYCN* amplified *nipbl* deactivated neuroblastoma model. Sexl M.

After analyzing the phenotypes of *nipbl* mutations, the Look laboratory will perform an in cross of the F3 *nipbla1 +/-; nipblb1 +/-;MYCN*-positive fish. This newly established zebrafish model can then be used to further study and elucidate the role of *nipbl* in *MYCN*-driven neuroblastoma.

All for this project proposed methods have already been established in the Look or other Laboratories (5–7,35,65–67,69,70).

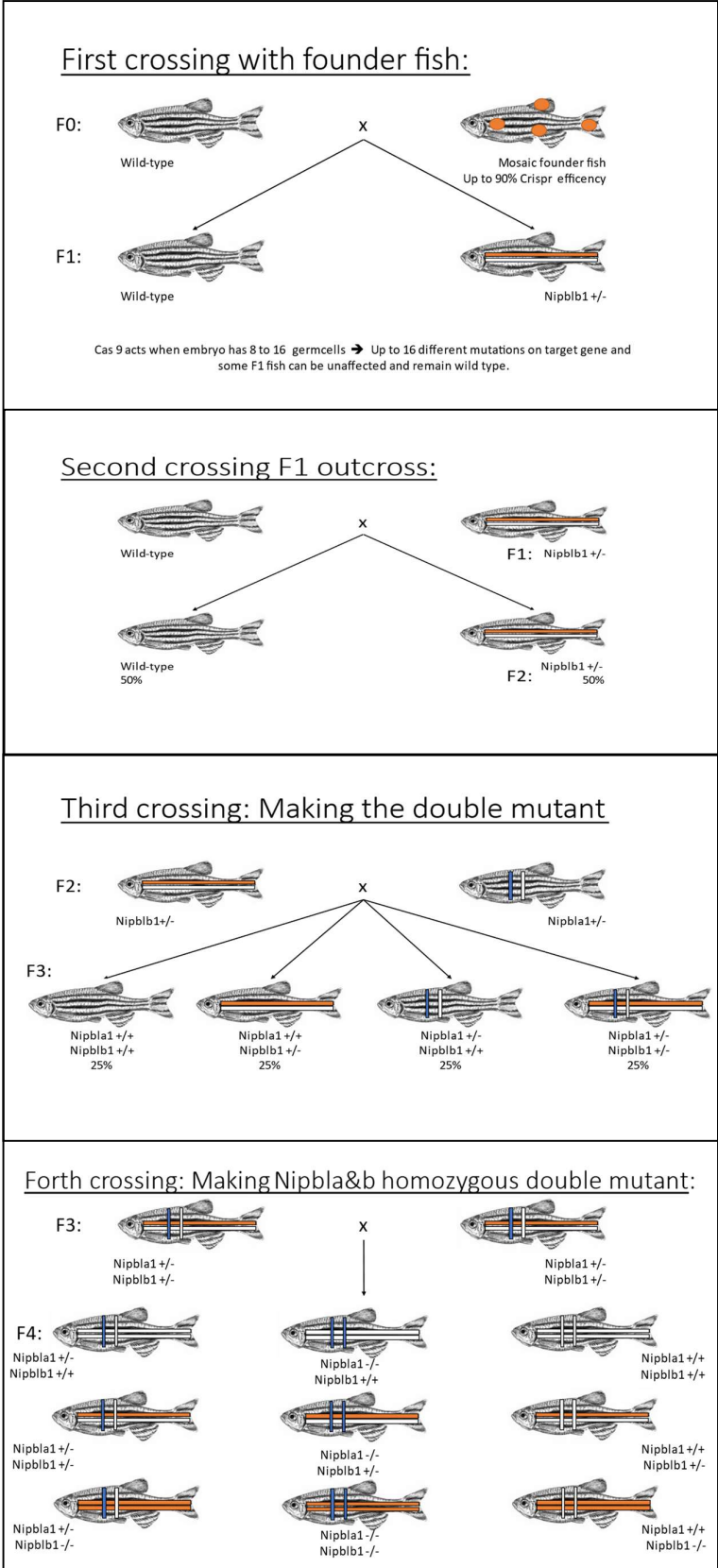


Figure 4: Schematic representation of breeding strategy. The in the second breeding introduced MYCN amplification is not shown

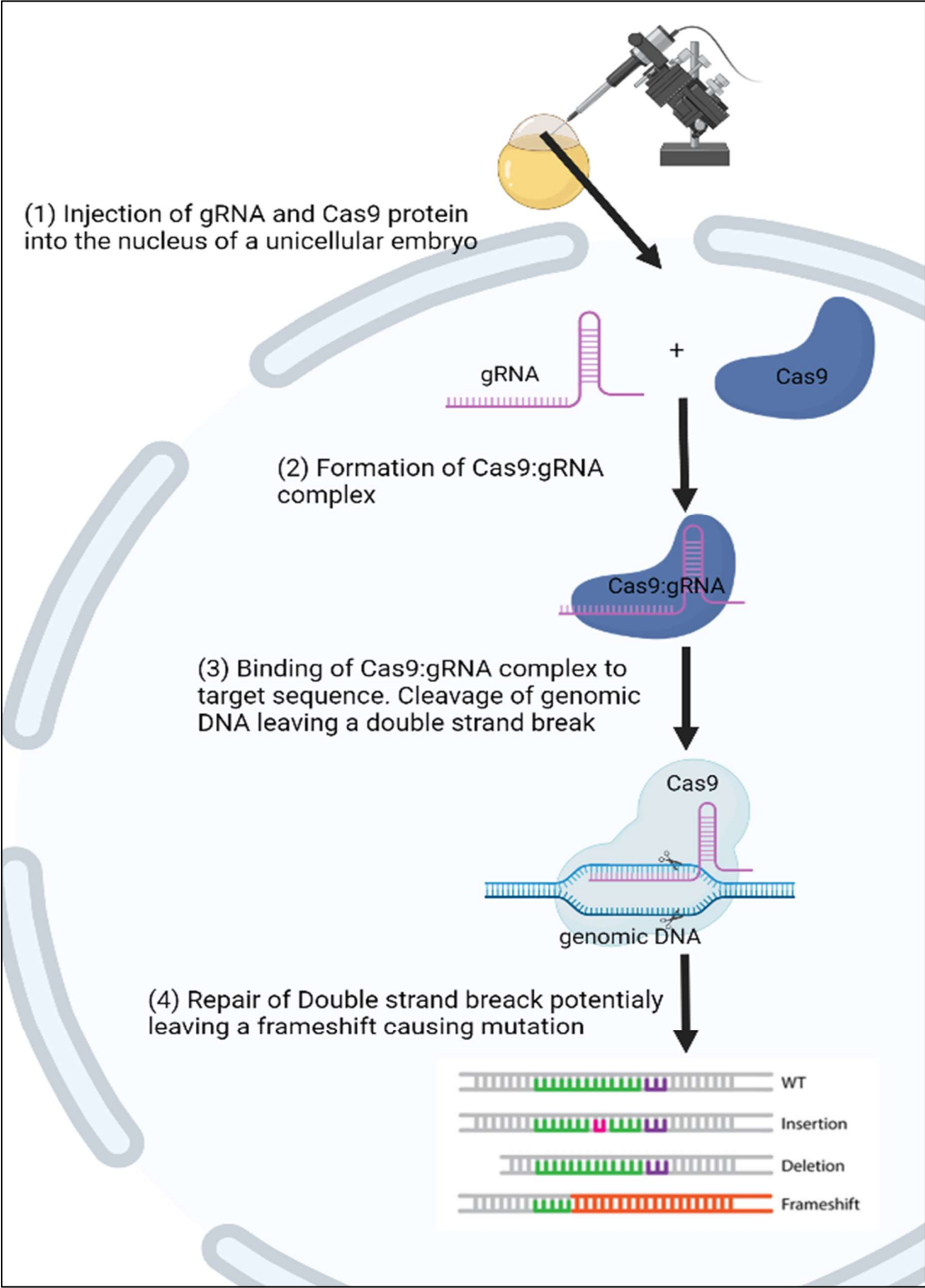


Figure 5: Schematic representation of Cas 9 mediated cleavage after its injection into the nucleus of an unicellular zebrafish embryo. This figure was made with BioRender.

Design of CRISPR/Cas 9 constructs :

As mentioned above a CRISPR/Cas 9 system was used to induce mutations in unicellular zebrafish. To assure that the mutations caused by the CRISPR system will effectively deactivate the targeted *nipbl* gene the constructs needed to be carefully designed.

A deactivating mutation of a gene has to result in the inability of the transcribed protein to perform its task. In this project early exons of the *nipbl* gene were targeted to create a frame shifting mutation. Mutations that do not shift the reading frame frequently do not change the transcribed protein enough to inhibit its action. To create a shift in the reading frame of a gene the mutation has to result in the net addition or deletion of a number of bases that is not a multiple of 3. The protein encoded by the mutated gene will then differ from the wild-type protein from the frame shifts position on (See figure 11). The earlier the mutation is placed in the genes coding regions the more the resulting protein will differ from the wild-type protein. It is therefore best to design your CRISPR systems to target an early exon of the target gene.

All the CRISPR constructs used for this project target an early exon of either *nipbla* or *nipblb*. The design of the CRISPR constructs used during this project can be seen in figure 6, 7, 8 and 9

The zebrafish as *MYCN* amplified *nipbl* deactivated neuroblastoma model. Sexl M.

```
TAGATGCTATCTGTCTCTTATAATGCTTCTCTACGTGGCAGCTAGTGTACATAGAAATCAATACACCTGTTAC
AGACAGTGAGTCTGAGTGGATTCTGCCAGGAAGCATAGTGTCTGTTAATAAATGACTGTAAAAGTTATGTTAA
TCTATTTAGGAAGAAGTCCGTACAAAACAAATGAGGCCGTGAAGATGAAATCCCATGTACTAAAACATTTTT
TCCCCTTCTTTAGGATTGAGTGAATGAGGGATGGTCAGCGAATAAATATCTCTGTGGATCTCTGTGTGC
GTTAGACTTCTGTGCCAGCCGTCAGTATGAATGGGGACATGCCACATGTGCCATTACAACCCTTGCTGGGA
TCGCTGGTCTCACTGACTGTAAGTACATGCATCAGATTACTCATGCTTCATTCTGTCTGTGCAGTCTCCGCC
CACTTTTTCAGCGGGATTGGTTTAAAAACAATATCCCATTCGTTTGTTCATTGTCAGGAACCATGCAAAACA
TCGCAGTCCCTTTGTTTTGAAGCGTAAAAACCACTGTTTACATTCTTTAATATTTTATTGAACAATTTATAAAC
GATGCAAATTTGTGATTTTTATTTATTTGTTTGTTCGTTGCTTGTTCGTTTATTTCATTCTTGTCTTTTT
CCCTCAATTTTTTTGGATCACATTGTAATAACAATGAAACAAAACAAGTTTCAGTGAAGTTAATGGAGTTTT
TTTCTGTAAGTTGAGTTTTTCAGGAACCCTTTTTGAAGGAATCTTTACATT
```

CRISPR construct 1 target:
GTGCCATTACAACCCTTGC

Sequence primer 1a: nipbla-F407, TCTGAGTGGATTCTGCCAGG
Sequence primer 1b: nipbla-R407, TGAAACAAACGAATGGGATATTGT

Figure 6: Partial genomic sequence of zebrafish *nipbla*. Exon 2 is highlighted in orange. CRISPR construct 1 is designed to target the underlined sequence (GTGCCATTACAACCCTTGC) possibly deactivating the gene. The sequence of the primers designed to replicate the genomic target region of CRISPR construct 1 is highlighted in blue. They bind to the sequence highlighted in yellow and enable the DNA polymerase to replicate the sequence in between those yellow highlighted parts. After a PCR we end up with a approximately 360 bp sequence containing the region targeted by CRISPR construct 1.

```
nipbla: exon6
CTTTGTTACATTTTGGGATTGTTTTGGAACCTCTAATTCAGTTGCCTGTGGGAGACATGACTAGGAATTGCAA
ATGCCAGAAATTGTCAAACACTTGTCTTACAAACAAGTGTGTTTCATGACTATACATAAAAAGTAAAATAATA
GAATAAGAAAATATGAGCTTCCAATCAAGCGGTGTAACGAGCTGTTTTTATCATCTAATAATCAATGGAAGTG
AATGAGAGCGGA GCCCAGAAGTTCCAATTCAAATGT GAAGAATAAGGTCAATAAACTGGATTTGAAGTGTA
ACCTCATAGATTTAATAGAATGTTGACCATGTCTCTCTGTTCTCTGTTCTGTTTATG CATTGTTGTACCGGGCCAG
TCTGTGCTCCTGGTGGACGGTTCTTCTCAGCAGGGCAGTCCAGTGGCCAGCCATATGCCCCAGAGCCCTG
CTACTGGTTACAGACAGTACCCTCACCCCTCAGCCTATAGTCAACACCAGCACCTACAGCAAGGTGTGCACAA
ACACACACACACACTGGAAGACCTGTATAGCAACTTCTTCATGCATCTGGTTTTTATTTCAGTTCTTGGGCT
CATTTTTTTTTTCTTCTTCCCTTAG GTTCAGTAGCAAGTCCCATGATCCAGGAGCCATGAGAAATGTGCATG
AAAATAAGGTATGTTGAAGTCTGATCTAGGGCTGTTTTTATACATTGCATAGATGCATATGCATACAGGCAGA
GATCGCATATCACACAGAAGCATTAAGGAGCACAACTTGTGAGTGTGCTGCTTGGGCTTTTTATTGATAAAAT
ATCTTTGCTTTTGAATGCATCATATTTCTCTGCAAC
```

CRISPR construct 2 target:
ACCGTCCACCAGGACCAGAC

Sequence primer 2a: nipbla-F416, GCCCAGAAGTTCCAATTCAAATGT
Sequence primer 2b: nipbla-R416, TCTCATGGCTCCTGGGATCA

Figure 7: Partial genomic sequence of zebrafish *nipbla*. Exon 6 is highlighted in orange. CRISPR construct 2 is designed to target the underlined sequence (GTCTGGTCTCCTGGTGGACGGT) possibly deactivating the gene. The sequence of the primers designed to replicate the genomic target region of CRISPR construct 2 is highlighted in blue. They bind to the sequence highlighted in yellow and enable the DNA polymerase to replicate the sequence in between those yellow highlighted parts. After a PCR we end up with a approximately 370 bp sequence containing the region targeted by CRISPR construct 2.

```
nipblb: exon7
```

The zebrafish as *MYCN* amplified *nipbl* deactivated neuroblastoma model. Sexl M.

CAAATAGAGAAATGCACTGCAAAATAGCACAGACTACAACGAAAACCTGTTTGGGAACCCCGAAAAGCTTTGTCCATTG
TTTTTTTTGTTTTGTTTTTTTTTAAAGATATTTTTGTTTATTTTATGGAGATACAAATAATAAACATTAATTCTTCT
CCCACTAAACATGTGCATAGAAGTACTCACACACATGCAAATACAGAATTGCACTGCAAAATAGCATAGACAACAAC
GAAAATGTGTGCGGGGACCCACAAAAGTTTATAGATCATATGGAGATGCACTCCACGGCAGAATCATCCAAATGA
TCTAACATTATAACTTCTTTCCAAATAGAGATATAAACTCATATGGTGAATTGTATTTCAGATCGTAATATATATAG
CAAAGTAAAAAAAATCTAGCAATAATAGATTTTTCCAATATGTGCAGCCCTACTTTTTATGTTTTATATA **TGCTC**
CTTATTGTGATCAATGCAAATAAAATGAAAACAGCAAATAAGTTGTCGTTTTCTGTTACAG **TTTCCGTATCCAGTCCA**
ATAGTTCCAGCGGCATGAGAAACATTACGACAACAAGTCTCTGGTCAAGTGTGGGTAACTCCAACCACAACGC
GAGGCATTGCTCCAGCGACGAGTACATCAACATCGTCCAGAGACTTGGAATGATGTGAGTGCTTGCCAAAGCTAAC
AGAAGATTTTATAACCCTAAATATATTACTCTTTTTAATCTTTTTATTAATTCGGCTGTGCCTAGGCCGTATATAT
GGCATAATTGTCCACCCGTGTTCTCTGTGTTTTACAG **GAGGGTGACCCCGCCATGAGAAATACCTCTTTCTCTGTA**
CGTCCGCTGTTCTCCTGCTGGAAGTGAAGGACTCCAAAAGGTGCATTAAACCTTAATTTGTAGCAATTTTATAT
AGCAACGTGCTTTTAGGTTCTTCCTTCCTTCACTTTTTACATTATATTTATGGTGTCTTTACACCATCCATGTGAGT
ACTGGCAGTGTTTACTAGCAGCAGCTGTGCACTACCGTAACAAGGTAACAACCTAAGGGTAAGATAATGCCAGATACA
CTGTTTAATTCATGTTATTGTCACTTTAAATATGCGCTCAGTACACAAACGCTGTGCTTGTCTGTTATGGATGTTT
AGCATGAGTATGCAATATAGACATACCATTTACTATGAACCACAAATATTTGTGTATGAGGCATACCTGAATCATAG
ATAAGTTATGCTTAGCCAAACTTTTCCA

CRISPR construct 3 target:
GTA ACTCCA ACCCAACGCG

Sequence primer 3a: nipblb-F428, **TGCTCCTTATTGTGATCAATGCAA**
Sequence primer 3b: nipblb-R428, **GGAGTCCCTTCACTTCCAGC**

Figure 8: Partial genomic sequence of zebrafish nipbl. Exon 7 is highlighted in orange. CRISPR construct 3 is designed to target the underlined sequence (GTA ACTCCA ACCCAACGCG) possibly deactivating the gene. The sequence of the primers designed to replicate the genomic target region of CRISPR construct 3 is highlighted in blue. They bind to the sequence highlighted in yellow and enable the DNA polymerase to replicate the sequence in between those yellow highlighted parts. After a PCR we end up with a approximately 380 bp sequence containing the region targeted by CRISPR construct 3.

```
nipblb: exon6
CTAGTACCGATAGTAGAACTGTATATGTCAGAGCTTTATTGATACTTCGGGCTTTTATTATTTAGCACCAATACCGA
TAAAGTACAGAGTTTCGGTACCCATCTCATAATGCCAGAATGACAATATAATTTACAAATCAAGTGCACCTTTACA
AAGAACACATTATATTTATTCTTCAGAATATTTAATTTAATATAGACATTTTTACAAGTTAATCAGGCATTGAAAT
CAGAATGTGAAAGCGCATATCCTAAATAAATAATGATATAAAACAAAAAATGCCAGGTAAAAAGTAAGAGGGTGCGA
TATCTGTACCAGATCAATTTCCATGTGTGTCAGACACCCAGTGAATAATATACTATAGTAATTTATAGTAAACTCTAT
AGTGTTTTTAACCATACTGACGCCTCCGATAGAGATAGAGATGTCGATATAAGTCGATATATTGATTATTGTGACAG
GCCTATTCGATAACACCATAACCAATCTACCTGCAGTGATTAAAAGAATTACAATATGCTGAAAATGAAAGTGTTAC
ATTTCAAGACTGATTACTGACCAGTTTCACTCTTGCTCCACAGCCGATATGTTCAAACCTCAGGCGGGTCTGGTAGC
AGGTACATGCCCCAGCAGAACAGTCCAGTGCCAGTCCGTATGCACCACAAAGTCCCGCGGGCTACATGCAGTACAG
CCACCCACCCAGCTACCCCCAGCACCAACCGATCCAGCAAGGTGAGTGCACATTCTCCTCTGTGAGACCCCAAGAG
GATTGTACCATTTTTGGCATCTATAGTCTTAAACCCTCAGGGCACAAGGAAAAGTGGTTTTAATAGGATTTTTG
CCTATTGAAGCTTCTTTTATCCATGTCTCTTGCTGAATAATGCAACTGATGATCCCATGATGTAAAAATAAATAAA
TAAATCTGTATTTACCTTCTAAAGGGATAGTTTGCTCAAAAAAGGATAATTCTGTGCATCATTTACTCTTCTTTAC
TTGTTTTAAACCTGTTTGACTTCTTCTGTGTAACACAAAGAAAGATACACTGTAAAACACCATTGGCTTCCAAAGT
AAAGGGTGAATTTACTAACATTTTATTCTGTTATTCTCTGAGCCTCGTGTGTTTATGAAACACATGATAGATAT
TTTCAATAAAACCATAAAGATTTTAGTCTTCTGTTGAAAGTCTTTTTACTTAAACTCTTAAACACACAACATGTTT
ATAGAAAATTATAGAATAATCCATATCAATCGAGTACGTTAATTAACCTTCTGATCATTTTGAGACATTTGTACAC
AAATATCATTTAACAGTGTTTCGCAGCATTTATATTGGCTCACAGAATCTTAGGCATGCTTGCTTGACGTGA
```

CRISPR construct 4 target:
GTATGCACCACAAAGTCCCG

Sequence primer 4a: nipblb-F420, ACCTGCAGTGATTAAAAGAATTACA
Sequence primer 4b: nipblb-R420, CATCATGGGATCATCAGTTGCATT

Figure 9: Partial genomic sequence of zebrafish *nipblb*. Exon 7 is highlighted in orange. CRISPR construct 4 is designed to target the underlined sequence (GTATGCACCACAAAGTCCCG) possibly deactivating the gene. The sequence of the primers designed to replicate the genomic target region of CRISPR construct 4 is highlighted in blue. They bind to the sequence highlighted in yellow and enable the DNA polymerase to replicate the sequence in between those yellow highlighted parts. After a PCR we end up with a approximately 370 bp sequence containing the region targeted by CRISPR construct 4.

Crossing and raising of fish

The crossing and raising of fish is an essential part of this project. To allow growth and sexual activity of the fish, they have to be held in conditions that resemble the conditions of their natural environment.

In nature, zebrafish can be found South Asia where they inhabit moderately flowing to stagnant clear water. The waters in which they live, mostly have a neutral to slightly basic pH and a temperature around 30°C. To replicate those conditions, the zebrafish in a system of constantly flowing water. The water is monitored and always has to have a temperature of 30°C and a pH of 7. Additionally the rooms containing the zebrafish are heated to a constant 28°C room temperature. The waterflow is controlled so that the fish do not have difficulties to swim against the current but have sufficient fresh water to keep the tank clean. To replicate the day night cycle the lights of the fish facility were turned on only in between 9h and 21h.

After the fish reach sexual maturity, they were crossed on a weekly basis. The fish meant to procreate were introduced into a Breeding tank filled with fresh system water. The breeding tank consist of the main tank and a removable insides with holes that permit the eggs to fall through. The fish were left overnight to get used to their environment. To increase the chance of mating, the insert was lifted and tilted creating a slope in the tank. This gives the zebrafish the impression to be near the shore of their habitat were it is safer for fish to hatch. As zebrafish consume their own eggs after laying the insert separating the fish from the eggs is essential. 6h after crossing the fish the eggs were collected and sorted. Only fertilized eggs with a chance to hatch were kept and treated with methylene blue to kill potential fungi growing on their surface. The fish were kept in this solution for 1 week until they were introduced into a rotifer rich system water solution.

4. Results :

4.1 Injection of CRISPR Construct :

The injection of CRISPR constructs into the unicellular fish was done by my colleague Shuning He. The injected fish were then tail clipped and genotyped by PCR, T-7 endonuclease I assay and sequencing.

The identified possible founder fish were then crossed with wild type fish (see figure ...) and their offspring was raised. Each founder fish can give birth to fish with up to 16 possible *nipbl* gene mutations. The offspring was genotyped and their sequences were analyzed. The overall efficiency of the CRISPR injection was high (around 80%) in the founder fish. Around 30% from the F0 wild type crossing stemming fish showed a mutation in the targeted *nipbl* gene suggesting that a high amount of germ cells were reached by the CRISPR construct. This suggestion is also supported by a high diversity in mutations found in the offspring of a single founder fish.

F1 analysis of Nipbla (CRISPR 1, Founder C)

| | | | |
|----------------|--|--------------|------|
| WT: | ACCCTTGCTGGGATCGCTGGTCTCACTGACTTGTGAACCAGCTGCCCTGCCCTCCC - | | |
| Mut1 (-4, +0): | ACCCT----GGGATCGCTGGTCTCACTGACTTGTGAACCAGCTGCC | out of frame | N=11 |
| Mut2 (-1, +0): | ACCCT-GCTGGGATCGCTGGTCTCACTGACTTGTGAACCAGCTGCC | out of frame | N=3 |
| Mut3 (-2, +0): | ACC--TGCTGGGATCGCTGGTCTCACTGACTTGTGAACCAGCTGCC | out of frame | N=8 |
| Mut4 (-7, +0): | ACCCT-----ATCGCTGGTCTCACTGACTTGTGAACCAGCTGCC | out of frame | N=1 |
| Mut5 (-6, +0): | AC-----TGGGATCGCTGGTCTCACTGACTTGTGAACCAGCTGCC | in frame | N=1 |

} 63 F1s sequenced,
29 mutants identified

Mut 1: 1; 27; 34; 35; 36; 47; 51; 55; 60; 67; 89
 Mut 2: 28; 53; 64
 Mut 3: 57; 75; 77; 81; 85; 87; 90; 96
 Mut 4: 62
 Mut 5: 68

Figure 10: F1 analysis of fish derived from founder fishes targeted by the CRISPR construct 1. Out of 63 suspected mutants after a T-7 endonuclease I assay 29 mutants could be confirmed via sequencing. 28 mutants had a frameshift causing mutation and were used for further breeding.

4.2 Selection of mutants :

After identifying F1 mutants, multiple zebrafish were selected for every CRISPR construct to complete the project. The zebrafish were all frame shifted *nipbl* mutants.

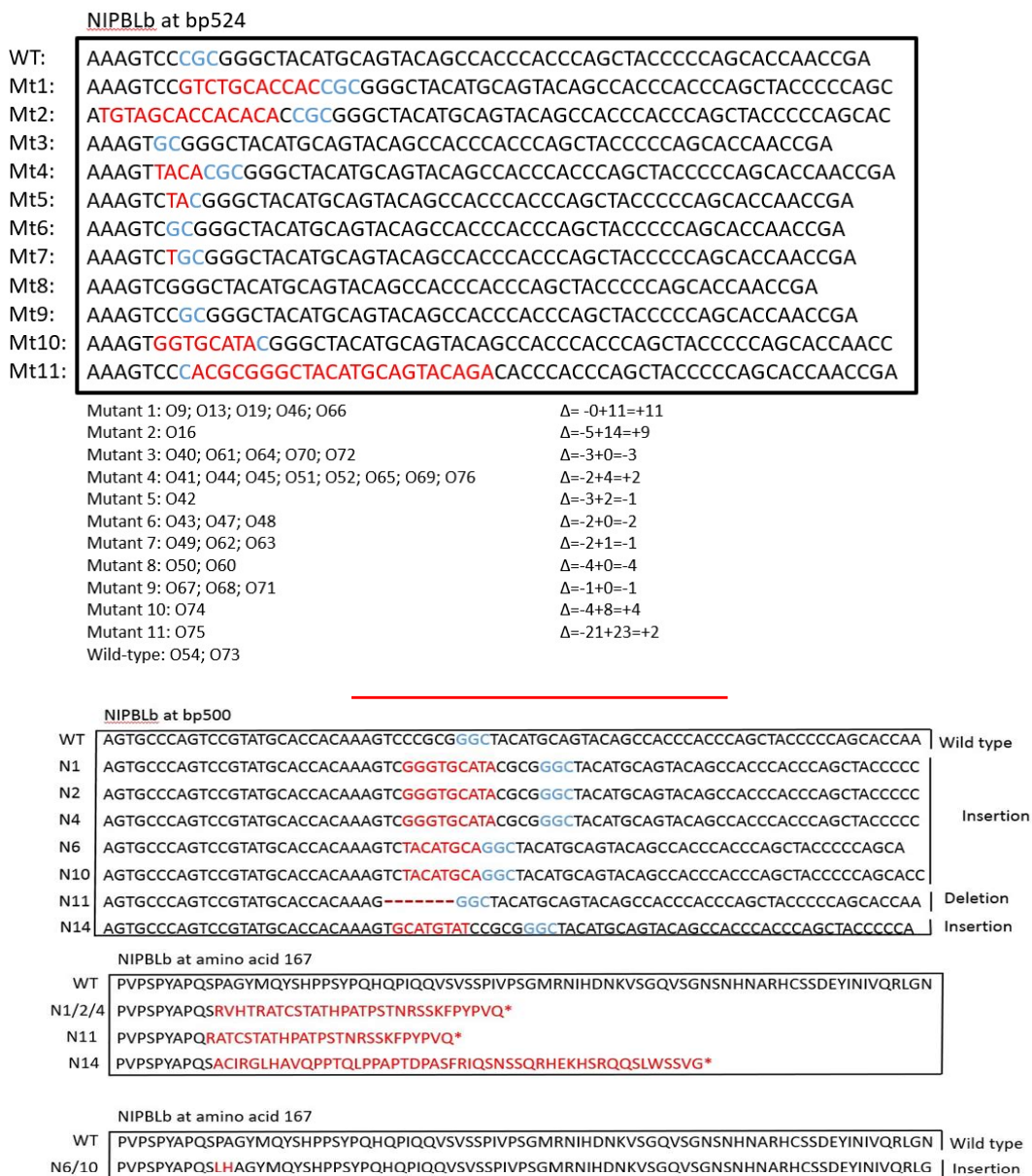


Figure 11: F1 analysis of fish derived from founder fishes targeted by the CRISPR construct 4

4.3 Breeding of mutants

The breeding of mutants has not been completed. Nipbla mutants will be crossed with Nipbl mutants generating the first generation of mutants with a possible inactivation of one allele of both *nipbl* genes. These fish once grown will be selected for mutations to identify the *nipbl* haploinsufficient fish. Look, He and colleagues can subsequently study tumor onset and initiation in those fish (see 7. Conclusion and Outlook).

5. Discussion :

In this project, we used zebrafish to establish a model of *MYCN* amplified, *nipbl* deactivated neuroblastoma. We have shown that the mutants selected in this project have frameshifting mutations within an early exon of the *nipbl* gene.

Teleost fishes have undergone whole genome duplication over 300 million years ago. Many of the duplicated genes have been lost over times but *nipbl* is still present in two copies. Genes that are still present in two copies are often expressed tissue specifically and are therefore both essential for the fish. It is not known if this is the case for the *nipbl* genes, it is also not known if one of the copies expression differs from the other. To replicate the loss of one *Nipbl* allele in humans, the zebrafish needs to lose two alleles. Because of the above mentioned tendency of duplicated genes being expressed tissue specifically one allele of each gene must be deactivated. While breeding the F1 and F2 generations we also inbred *nipbla* deactivated fish with *nipbla* deactivated fish and *nipblb* deactivated fish with *nipblb* deactivated fish to generate a *nipbla* *-/-*; *nipblb* *+/+* and a *nipbla* *+/+*; *nipblb* *-/-* populations. The by the breeding generated zebrafish were genotyped and selected for mutation. The *nipbla* *-/-* ; *nipblb* *+/+* and *nipbla* *+/+* ; *nipblb* *-/-* populations both did not show any by the blank eye visible phenotypes. As a complete knockout of *nipbl* is embryonic lethal, the survival of the *nipbla* *-/-* ; *nipblb* *+/+* and *nipbla* *+/+* ; *nipblb* *-/-* populations indicates that the complete loss of one *nipbl* gene is at least partially compensated by the other in all tissues.

As the complete loss of cohesin is embryonic lethal, most disease associated mutations of the cohesin complex are haploinsufficient. The only exception to this rule are the cohesin subunits *STAG2* and *SMC1A* as *STAG2* is partially compensated by *STAG1* also a subunit of cohesin(71). The diseases associated to a mutation of one of the cohesin genes are collectively known as the “cohesinopathies” (72). Cohesinopathies present similar but different phenotypes

depending on which cohesin subunit or loader is mutated. The best known cohesinopathies is the Cornelia de Lange syndrome (CdLS). 70% of CdLS patients present a dominant mutation of one of the *nipbl* genes leading to the most severe of CdLS(73)(74). These patients suffer from severe physical and mental developmental retardation causing speech and language delay, attention deficit disorder, hyperactivity, growth retardation, limb deformation and cranial and skeletal anomalies(75,76). Patients suffering from Robert's syndrome a rare autosomal recessive disorder caused by mutations of the gene encoding ESCO2 a cohesin complex regulator present similar very similar phenotypes with few exceptions. The same can be said for other rare and even less documented cohesinopathies like Warsaw breakage syndrome(77,78). To understand cohesin related diseases it is imperative to investigate more into the role cohesin plays not only in the shaping of the 3D genome but also in DNA repair where it has been found to play a crucial role in double stranded DNA break repair(46–48).

Besides cohesinopathies, mutations of one of the cohesin complex genes are associated with a wide range of cancer. Somatic mutations have been found in patients of glioblastoma (4–6%), Ewing's sarcoma (17–20%), bladder (11–36%) and myeloid neoplasms (13%). Interestingly no specific mutation hotspots could be found and mutations can be found in many of the cohesin genes and regulators. The prognostic impact of a mutation in one of the cohesin genes is still discussed as it has been associated with favorable, insignificant and unfavorable impact on patient survival of myeloid leukemia(79). Due to the cell-type specific expression of the cohesin ring, it is expected that the prognostic impact may vary vastly in between cancerous cell-types. At the same time its involvement in multiple diseases makes it a viable target for therapeutics. Currently about 20 chemical agents are known that potentially target the cohesin complex or one of its regulators(80).

This project really highlighted the advantages of zebrafish mentioned briefly above. The handling of zebrafish can be done with extreme ease. Staff that has never worked with zebrafish can quickly learn how to handle the fish and how to

The zebrafish as *MYCN* amplified *nipbl* deactivated neuroblastoma model. Sexl M.

work with them in an efficient way. This project was very genotyping intensive as every fish has to be checked for mutations of *nipbl* and if one is present the sample needs to be sequenced. After a short time working and getting used to zebrafish one single member of staff is able to genotype and sequence around 100 fish every three days without delay. This is in part made possible by the use of tricaine as a sedative and the incredible quick procedure of tail clipping. To sedate and clip the tail of a single fish no more than 2 minutes is needed. Working in synergy with the easy handling of zebrafish is their high reproductive ability. Throughout the project one single member of staff was responsible for the set-up of mating and juvenile care of the *nipbl* mutants. During periods of high reproductions up to 700 eggs were collected a week. Upon hatching from their eggs zebrafish are very small and can therefore be kept in groups of around 50. After two weeks the fish were separated into groups of 15 fish. This allowed us to keep a high amount of fish on a relatively small space (3L water for 15 fish).

6. Conclusion & Outlook :

This project was aimed to establish a *MYCN* amplified, *nipbl* deactivated neuroblastoma. This neuroblastoma model consist of two different *nipbl* deactivated fish populations: One with a frameshifting mutation in exon 2 of one allele of *nipbla* and a frameshifting mutation in exon 7 of one allele of *nipblb* and another with a frameshifting mutation in exon 6 of one allele of *nipbla* and a frameshifting mutation in exon 6 of one allele of *nipblb*. At the moment of this report the first population was whereas, the second population still needs to be generated. To establish the neuroblastoma model we followed the breeding program described in figure During the crossing of the F1 and the F2 generation we used *MYCN* transgenic fishes that have previously been selected for tumors. As the fish used for the injection were homozygous nacre mutants we could easily select for F2 and F3 fish with the *MYCN* transgene by checking for pigmentation. The *MYCN* amplified, *nipbl* deactivated can now be used for further experiments and studies about the mechanisms involved.

This project is part of a bigger project between the Dana-Farber Cancer Institute, the M.I.T. and St. Jude's research hospital. The first thing that must be done once both *MYCN* amplified, *nipbl* deactivated fish populations are established is to check for accelerated tumor onset of *nipbl* deactivated neuroblastoma. The production of EGFP by all neural crest cells is particularly easy to monitor. As mentioned above only tumors will have a large enough cell mass to produce sufficient EGFP for it to be visualized by UV and the naked eye.

MYCN amplified, *nipbl* deactivated zebrafish and *MYCN* amplified zebrafish will be monitored daily for tumor growth. We expect to observe an earlier onset of tumors in the *nipbl* deactivated fish as such mutations have previously been identified in neuroblastoma. *MYCN* amplified, *nipbl* deactivated fish will also be sacrificed at different timepoints to perform Immunohistochemical analysis of the tumor tissue and quantify the EGFP positive cells composing the tumor.

As the mechanisms underlying the loss of *nipbl* in neuroblastoma are largely unknown, investigation into genes that may be transcriptionally regulated by *nipbl* is essential. Many transcription factors bind to their target sequence or a sequence that is adjacent to their target. *Nipbl* and the cohesin ring do not regulate genes by binding to them directly but shape chromatin to form loops that are more or less exposed to the transcriptional machinery. The cohesin ring can therefore regulate a gene even if it is multiple kb away from the CTCF site that stops the loop extrusion through the cohesin ring complex. Cohesin rings are essential for mammalian organisms to develop correctly and shapes the 3D genome in the vast majority of human cells. Cohesin is therefore expected to regulate a vast array of genes. Large gene expression screens could prove useful to check for gene expression levels that differ in wild-type and *nipbl* deficient cells and animals.

References :

1. Cancer Incidence and Survival Among Children and Adolescents: United States ... - Google Books [Internet]. [cited 2022 Jan 5]. Available from: <https://books.google.com/books?hl=en&lr=&id=LaxAFksCV6gC&oi=fnd&pg=PR3&ots=rywXuSNXgq&sig=5kSiYQBZ5UI6i1S8K0g-UsmMgAqE#v=onepage&q&f=false>
2. Tomolonis JA, Agarwal S, Shohet JM. Neuroblastoma pathogenesis: deregulation of embryonic neural crest development. *Cell Tissue Res* [Internet]. 2018 May 1 [cited 2022 Jan 5];372(2):245. Available from: </pmc/articles/PMC5918240/>
3. Twist CJ, Schmidt M lou, Naranjo A, London WB, Tenney SC, Marachelian A, et al. Maintaining Outstanding Outcomes Using Response- and Biology-Based Therapy for Intermediate-Risk Neuroblastoma: A Report From the Children's Oncology Group Study ANBL0531. *Journal of Clinical Oncology* [Internet]. 2019 [cited 2022 Jan 5];37(34):3243. Available from: </pmc/articles/PMC6881103/>
4. Mlakar V, Jurkovic Mlakar S, Lopez G, Maris JM, Ansari M, Gumy-Pause F. 11q deletion in neuroblastoma: a review of biological and clinical implications. *Molecular Cancer* [Internet]. 2017 Jun 29 [cited 2022 Jan 5];16(1). Available from: </pmc/articles/PMC5492892/>
5. Zhu S, Thomas Look A. Neuroblastoma and its zebrafish model. In: *Advances in Experimental Medicine and Biology*. Springer New York LLC; 2016. p. 451–78.
6. 324 -He Sh & A.Thomas Look eLife-2016.
7. Zhu S, Lee JS, Guo F, Shin J, Perez-Atayde AR, Kutok JL, et al. Activated ALK Collaborates with MYCN in Neuroblastoma Pathogenesis. *Cancer Cell*. 2012 Mar 20;21(3):362–73.
8. Matthay KK, Maris JM, Schleiermacher G, Nakagawara A, Mackall CL, Diller L, et al. Neuroblastoma. *Nat Rev Dis Primers* [Internet]. 2016 Nov 10 [cited 2022 Jan 5];2. Available from: <https://pubmed.ncbi.nlm.nih.gov/27830764/>
9. Park JR, Kreissman SG, London WB, Naranjo A, Cohn SL, Hogarty MD, et al. Effect of Tandem Autologous Stem Cell Transplant vs Single Transplant on Event-Free Survival in Patients With High-Risk Neuroblastoma: A Randomized Clinical Trial. *JAMA* [Internet]. 2019 Aug 27 [cited 2022 Jan 5];322(8):746. Available from: </pmc/articles/PMC6714031/>
10. Tonini GP, Capasso M. Genetic predisposition and chromosome instability in neuroblastoma. *Cancer Metastasis Rev* [Internet]. 2020 Mar 1 [cited 2022 Jan 5];39(1):275–85. Available from: <https://pubmed.ncbi.nlm.nih.gov/31927719/>
11. Gatta G, Botta L, Rossi S, Aareleid T, Bielska-Lasota M, Clavel J, et al. Childhood cancer survival in Europe 1999-2007: results of EURO CARE-5--a population-based study. *Lancet Oncol* [Internet]. 2014 Jan [cited 2022 Jan 5];15(1):35–47. Available from: <https://pubmed.ncbi.nlm.nih.gov/24314616/>
12. Strother DR, London WB, Schmidt M lou, Brodeur GM, Shimada H, Thorner P, et al. Outcome after surgery alone or with restricted use of chemotherapy for patients with low-

- risk neuroblastoma: results of Children's Oncology Group study P9641. *J Clin Oncol* [Internet]. 2012 May 20 [cited 2022 Jan 5];30(15):1842–8. Available from: <https://pubmed.ncbi.nlm.nih.gov/22529259/>
13. Baker DL, Schmidt ML, Cohn SL, Maris JM, London WB, Buxton A, et al. Outcome after Reduced Chemotherapy for Intermediate-Risk Neuroblastoma. *New England Journal of Medicine* [Internet]. 2010 Sep 30 [cited 2022 Jan 5];363(14):1313–23. Available from: <https://www.nejm.org/doi/full/10.1056/nejmoa1001527>
 14. Maris JM, Hogarty MD, Bagatell R, Cohn SL. Neuroblastoma. *Lancet* [Internet]. 2007 Jun 23 [cited 2022 Jan 5];369(9579):2106–20. Available from: <https://pubmed.ncbi.nlm.nih.gov/17586306/>
 15. Tolbert VP, Matthay KK. Neuroblastoma: Clinical and Biological Approach to Risk Stratification and Treatment. *Cell Tissue Res* [Internet]. 2018 May 1 [cited 2022 Jan 5];372(2):195. Available from: </pmc/articles/PMC5918153/>
 16. Finklestein JZ, Gilchrist GS. Recent Advances in Neuroblastoma. <http://dx.doi.org/101056/NEJMra0804577> [Internet]. 2010 Jun 4 [cited 2022 Jan 5];116(3):116–27. Available from: <https://www.nejm.org/doi/full/10.1056/NEJMra0804577>
 17. Brodeur GM. Neuroblastoma: biological insights into a clinical enigma. *Nat Rev Cancer* [Internet]. 2003 Mar [cited 2022 Jan 5];3(3):203–16. Available from: <https://pubmed.ncbi.nlm.nih.gov/12612655/>
 18. Otte J, Dyberg C, Pepich A, Johnsen JI. MYCN Function in Neuroblastoma Development. *Frontiers in Oncology*. 2021 Jan 27;10:3210.
 19. Dang C v. MYC on the path to cancer. *Cell* [Internet]. 2012 Mar 30 [cited 2022 Jan 5];149(1):22–35. Available from: <https://pubmed.ncbi.nlm.nih.gov/22464321/>
 20. Duffy MJ, O'Grady S, Tang M, Crown J. MYC as a target for cancer treatment. *Cancer Treatment Reviews* [Internet]. 2021 Mar 1 [cited 2022 May 8];94:102154. Available from: <http://www.cancertreatmentreviews.com/article/S0305737221000025/fulltext>
 21. Schaub F, Dhankani V, Berger A, systems MTC, 2018 undefined. Pan-cancer alterations of the MYC oncogene and its proximal network across the cancer genome atlas. Elsevier [Internet]. [cited 2022 May 8]; Available from: <https://www.sciencedirect.com/science/article/pii/S2405471218300978>
 22. Huang M, Weiss WA. Neuroblastoma and MYCN. *Cold Spring Harbor Perspectives in Medicine*. 2013;3(10).
 23. Ozer E, Altungoz O, Unlu M, Aygun N, Tumer S, Olgun N. Association of MYCN amplification and 1p deletion in neuroblastomas with high tumor vascularity. *Appl Immunohistochem Mol Morphol* [Internet]. 2007 Jun [cited 2022 Jan 11];15(2):181–6. Available from: <https://pubmed.ncbi.nlm.nih.gov/17525631/>
 24. Ribatti D, Raffaghello L, Pastorino F, Nico B, Brignole C, Vacca A, et al. In vivo angiogenic activity of neuroblastoma correlates with MYCN oncogene overexpression. *Int J Cancer*

- [Internet]. 2002 Dec 1 [cited 2022 Jan 11];102(4):351–4. Available from: <https://pubmed.ncbi.nlm.nih.gov/12402304/>
25. Meitar D, Crawford SE, Rademaker AW, Cohn SL. Tumor angiogenesis correlates with metastatic disease, N-myc amplification, and poor outcome in human neuroblastoma. <https://doi.org/10.1200/JCO.1996.14.2405>. 2016 Sep 21;14(2):405–14.
 26. Henriksen JR, Haug BH, Buechner J, Tømte E, Løkke C, Flaegstad T, et al. Conditional expression of retrovirally delivered anti-MYCN shRNA as an in vitro model system to study neuronal differentiation in MYCN-amplified neuroblastoma. *BMC Dev Biol* [Internet]. 2011 [cited 2022 Jan 11];11. Available from: <https://pubmed.ncbi.nlm.nih.gov/21194500/>
 27. Lovén J, Zinin N, Wahlström T, Müller I, Brodin P, Fredlund E, et al. MYCN-regulated microRNAs repress estrogen receptor-alpha (ESR1) expression and neuronal differentiation in human neuroblastoma. *Proc Natl Acad Sci U S A* [Internet]. 2010 Jan 26 [cited 2022 Jan 11];107(4):1553–8. Available from: <https://pubmed.ncbi.nlm.nih.gov/20080637/>
 28. Cotterman R, Knoepfler PS. N-Myc regulates expression of pluripotency genes in neuroblastoma including *lif*, *klf2*, *klf4*, and *lin28b*. *PLoS One* [Internet]. 2009 Jun 4 [cited 2022 Jan 11];4(6). Available from: <https://pubmed.ncbi.nlm.nih.gov/19495417/>
 29. Kang JH, Rychahou PG, Ishola TA, Qiao J, Evers BM, Chung DH. MYCN silencing induces differentiation and apoptosis in human neuroblastoma cells. *Biochem Biophys Res Commun* [Internet]. 2006 Dec 8 [cited 2022 Jan 11];351(1):192–7. Available from: <https://pubmed.ncbi.nlm.nih.gov/17055458/>
 30. Wakamatsu Y, Watanabe Y, Nakamura H, Kondoh H. Regulation of the neural crest cell fate by N-myc: promotion of ventral migration and neuronal differentiation. *Development*. 1997 May 15;124(10):1953–62.
 31. George RE, Sanda T, Hanna M, Fröhling S, Luther W, Zhang J, et al. Activating mutations in ALK provide a therapeutic target in neuroblastoma. *Nature* [Internet]. 2008 Oct 16 [cited 2022 Jan 5];455(7215):975–8. Available from: <https://pubmed.ncbi.nlm.nih.gov/18923525/>
 32. Mossé YP, Laudenslager M, Longo L, Cole KA, Wood A, Attiyeh EF, et al. Identification of ALK as a major familial neuroblastoma predisposition gene. *Nature* [Internet]. 2008 Oct 16 [cited 2022 Jan 5];455(7215):930–5. Available from: <https://pubmed.ncbi.nlm.nih.gov/18724359/>
 33. de Brouwer S, de Preter K, Kumps C, Zabrocki P, Porcu M, Westerhout EM, et al. Meta-analysis of neuroblastomas reveals a skewed ALK mutation spectrum in tumors with MYCN amplification. *Clin Cancer Res* [Internet]. 2010 Sep 1 [cited 2022 Jan 5];16(17):4353–62. Available from: <https://pubmed.ncbi.nlm.nih.gov/20719933/>
 34. Chang HH, Lu MY, Yang YL, Chou SW, Lin DT, Lin KH, et al. The prognostic roles of and correlation between ALK and MYCN protein expression in neuroblastoma. *J Clin Pathol* [Internet]. 2020 Mar 1 [cited 2022 Jan 5];73(3):154–61. Available from: <https://pubmed.ncbi.nlm.nih.gov/31542727/>

The zebrafish as *MYCN* amplified *nipbl* deactivated neuroblastoma model. Sexl M.

35. Morrison MA, Zimmerman MW, Look AT, Stewart RA. Studying the peripheral sympathetic nervous system and neuroblastoma in zebrafish. *Methods in Cell Biology*. 2016;134:97–138.
36. Gao D, Zhu B, Cao X, Zhang M, Wang X. Roles of NIPBL in maintenance of genome stability. *Seminars in Cell & Developmental Biology*. 2019 Jun 1;90:181–6.
37. Tonkin ET, Wang TJ, Lisgo S, Bamshad MJ, Strachan T. NIPBL, encoding a homolog of fungal Scc2-type sister chromatid cohesion proteins and fly Nipped-B, is mutated in Cornelia de Lange syndrome. *Nat Genet* [Internet]. 2004 Jun [cited 2022 Jan 4];36(6):636–41. Available from: <https://pubmed.ncbi.nlm.nih.gov/15146185/>
38. Shi Z, Gao H, Bai XC, Yu H. Cryo-EM structure of the human cohesin-NIPBL-DNA complex. *Science* [Internet]. 2020 Jun 26 [cited 2022 Jan 4];368(6498):1454–9. Available from: <https://pubmed.ncbi.nlm.nih.gov/32409525/>
39. Nasmyth K, Haering CH. Cohesin: its roles and mechanisms. *Annu Rev Genet* [Internet]. 2009 Dec 1 [cited 2022 Jan 4];43:525–58. Available from: <https://pubmed.ncbi.nlm.nih.gov/19886810/>
40. Kim Y, Shi Z, Zhang H, Finkelstein IJ, Yu H. Human cohesin compacts DNA by loop extrusion. *Science* [Internet]. 2019 Dec 13 [cited 2022 Jan 4];366(6471):1345. Available from: </pmc/articles/PMC7387118/>
41. Fritz AJ, Sehgal N, Pliss A, Xu J, Berezney R. Chromosome territories and the global regulation of the genome. *Genes Chromosomes Cancer* [Internet]. 2019 Jul 1 [cited 2022 Apr 16];58(7):407. Available from: </pmc/articles/PMC7032563/>
42. Bonev B, Cavalli G. Organization and function of the 3D genome. *Nat Rev Genet* [Internet]. 2016 Oct 14 [cited 2022 Apr 16];17(11):661–78. Available from: <https://pubmed.ncbi.nlm.nih.gov/27739532/>
43. Krijger PHL, de Laat W. Regulation of disease-associated gene expression in the 3D genome. *Nat Rev Mol Cell Biol* [Internet]. 2016 Nov 21 [cited 2022 Apr 16];17(12):771–82. Available from: <https://pubmed.ncbi.nlm.nih.gov/27826147/>
44. Kempfer R, Pombo A. Methods for mapping 3D chromosome architecture. *Nature Reviews Genetics* 2019 21:4 [Internet]. 2019 Dec 17 [cited 2022 Apr 16];21(4):207–26. Available from: <https://www.nature.com/articles/s41576-019-0195-2>
45. Ishiguro K ichiro. The cohesin complex in mammalian meiosis. *Genes Cells* [Internet]. 2019 Jan 1 [cited 2022 Apr 16];24(1):6–30. Available from: <https://pubmed.ncbi.nlm.nih.gov/30479058/>
46. Phipps J, Dubrana K. DNA Repair in Space and Time: Safeguarding the Genome with the Cohesin Complex. *Genes (Basel)* [Internet]. 2022 Feb 1 [cited 2022 Apr 15];13(2). Available from: <https://pubmed.ncbi.nlm.nih.gov/35205243/>
47. Arnould C, Rocher V, Finoux AL, Clouaire T, Li K, Zhou F, et al. Loop extrusion as a mechanism for formation of DNA damage repair foci. *Nature* [Internet]. 2021 Feb 25 [cited

- 2022 Apr 15];590(7847):660–5. Available from: <https://pubmed.ncbi.nlm.nih.gov/33597753/>
48. Tothova Z, Valton AL, Gorelov RA, Vallurupalli M, Krill-Burger JM, Holmes A, et al. Cohesin mutations alter DNA damage repair and chromatin structure and create therapeutic vulnerabilities in MDS/AML. *JCI Insight* [Internet]. 2021 Feb 8 [cited 2022 Apr 15];6(3). Available from: <https://pubmed.ncbi.nlm.nih.gov/33351783/>
 49. Heidinger-Pauli JM, Mert O, Davenport C, Guacci V, Koshland D. Systematic Reduction of Cohesin Differentially Affects Chromosome Segregation, Condensation, and DNA Repair. *Current Biology*. 2010 May 25;20(10):957–63.
 50. Seitan VC, Faure AJ, Zhan Y, McCord RP, Lajoie BR, Ing-Simmons E, et al. Cohesin-based chromatin interactions enable regulated gene expression within preexisting architectural compartments. *Genome Research* [Internet]. 2013 Dec [cited 2022 Apr 16];23(12):2066. Available from: </pmc/articles/PMC3847776/>
 51. Liu NQ, Maresca M, van den Brand T, Braccioli L, Schijns MMGA, Teunissen H, et al. WAPL maintains a cohesin loading cycle to preserve cell-type specific distal gene regulation. *Nat Genet* [Internet]. 2021 Jan 1 [cited 2022 May 8];53(1):100. Available from: </pmc/articles/PMC7610352/>
 52. Weiss WA, Aldape K, Mohapatra G, Feuerstein BG, Bishop JM. Targeted expression of *MYCN* causes neuroblastoma in transgenic mice. *The EMBO Journal* [Internet]. 1997 Jun 2 [cited 2022 Jan 6];16(11):2985. Available from: </pmc/articles/PMC1169917/?report=abstract>
 53. Howe K, Clark MD, Torroja CF, Torrance J, Berthelot C, Muffato M, et al. The zebrafish reference genome sequence and its relationship to the human genome. *Nature* [Internet]. 2013 Apr 25 [cited 2022 Jan 9];496(7446):498–503. Available from: <https://pubmed.ncbi.nlm.nih.gov/23594743/>
 54. Kettleborough RNW, Busch-Nentwich EM, Harvey SA, Dooley CM, de Bruijn E, van Eeden F, et al. A systematic genome-wide analysis of zebrafish protein-coding gene function. *Nature* [Internet]. 2013 Apr 25 [cited 2022 Jan 9];496(7446):494–7. Available from: <https://pubmed.ncbi.nlm.nih.gov/23594742/>
 55. Hwang KL, Goessling W. Baiting for Cancer: Using the Zebrafish as a Model in Liver and Pancreatic Cancer. *Adv Exp Med Biol* [Internet]. 2016 [cited 2022 Jan 11];916:391–410. Available from: <https://pubmed.ncbi.nlm.nih.gov/27165363/>
 56. He S, Jing CB, Look AT. Zebrafish models of leukemia. *Methods Cell Biol* [Internet]. 2017 [cited 2022 Jan 11];138:563–92. Available from: <https://pubmed.ncbi.nlm.nih.gov/28129858/>
 57. Botorabi F, Manouchehri H, Changizi R, Barker H, Palazzo E, Saltari A, et al. Zebrafish as a Model Organism for the Development of Drugs for Skin Cancer. *Int J Mol Sci* [Internet]. 2017 Jul 18 [cited 2022 Jan 11];18(7). Available from: <https://pubmed.ncbi.nlm.nih.gov/28718799/>

58. Amawi H, Aljabali AAA, Boddu SHS, Amawi S, Obeid MA, Ashby CR, et al. The use of zebrafish model in prostate cancer therapeutic development and discovery. *Cancer Chemother Pharmacol* [Internet]. 2021 Mar 1 [cited 2022 Jan 11];87(3):311–25. Available from: <https://pubmed.ncbi.nlm.nih.gov/33392639/>
59. Hwang WY, Fu Y, Reyon D, Maeder ML, Tsai SQ, Sander JD, et al. Efficient In Vivo Genome Editing Using RNA-Guided Nucleases. *Nat Biotechnol* [Internet]. 2013 Mar [cited 2022 Jan 4];31(3):227. Available from: </pmc/articles/PMC3686313/>
60. Terns MP, Terns RM. CRISPR-based adaptive immune systems. *Curr Opin Microbiol* [Internet]. 2011 Jun [cited 2022 Jan 4];14(3):321–7. Available from: <https://pubmed.ncbi.nlm.nih.gov/21531607/>
61. Horvath P, Barrangou R. CRISPR/Cas, the immune system of bacteria and archaea. *Science* [Internet]. 2010 [cited 2022 Jan 4];327(5962):167–70. Available from: <https://pubmed.ncbi.nlm.nih.gov/20056882/>
62. Doudna JA, Charpentier E. The new frontier of genome engineering with CRISPR-Cas9. *Science* (1979) [Internet]. 2014 Nov 28 [cited 2022 Jan 4];346(6213). Available from: <https://www.science.org/doi/abs/10.1126/science.1258096>
63. Westermann L, Neubauer B, Köttgen M. Nobel Prize 2020 in Chemistry honors CRISPR: a tool for rewriting the code of life. *Pflugers Archiv* [Internet]. 2021 Jan 1 [cited 2022 Jan 9];473(1):1. Available from: </pmc/articles/PMC7782372/>
64. Hsu PD, Lander ES, Zhang F. Development and applications of CRISPR-Cas9 for genome engineering. *Cell* [Internet]. 2014 Jun 5 [cited 2022 Jan 4];157(6):1262–78. Available from: <https://pubmed.ncbi.nlm.nih.gov/24906146/>
65. Hwang WY, Fu Y, Reyon D, Maeder ML, Tsai SQ, Sander JD, et al. Efficient genome editing in zebrafish using a CRISPR-Cas system. *Nat Biotechnol* [Internet]. 2013 Mar [cited 2022 Jan 4];31(3):227–9. Available from: <https://pubmed.ncbi.nlm.nih.gov/23360964/>
66. Albadri S, del Bene F, Revenu C. Genome editing using CRISPR/Cas9-based knock-in approaches in zebrafish. *Methods*. 2017 May 15;121–122:77–85.
67. Hoshijima K, Jurynek MJ, Klatt Shaw D, Jacobi AM, Behlke MA, Grunwald DJ. Highly efficient methods for generating deletion mutations and F0 embryos that lack gene function in zebrafish. *Dev Cell* [Internet]. 2019 Dec 2 [cited 2022 Jan 4];51(5):645. Available from: </pmc/articles/PMC6891219/>
68. Naeem M, Majeed S, Hoque MZ, Ahmad I. Latest Developed Strategies to Minimize the Off-Target Effects in CRISPR-Cas-Mediated Genome Editing. *Cells* [Internet]. 2020 Jul 2 [cited 2022 Jan 9];9(7). Available from: <https://pubmed.ncbi.nlm.nih.gov/32630835/>
69. Li S, Yeo KS, Levee TM, Howe CJ, Her ZP, Zhu S. Zebrafish as a Neuroblastoma Model: Progress Made, Promise for the Future. *Cells* [Internet]. 2021 Mar 1 [cited 2022 Jan 6];10(3):1–18. Available from: </pmc/articles/PMC8001113/>

70. Hua Y, Wang C, Huang J, Wang K. A simple and efficient method for CRISPR/Cas9-induced mutant screening. *J Genet Genomics* [Internet]. 2017 Apr 20 [cited 2022 Jan 4];44(4):207–13. Available from: <https://pubmed.ncbi.nlm.nih.gov/28416245/>
71. Adane B, Alexe G, Seong BKA, Lu D, Hwang EE, Hnisz D, et al. STAG2 loss rewires oncogenic and developmental programs to promote metastasis in Ewing sarcoma. *Cancer Cell* [Internet]. 2021 Jun 14 [cited 2022 Apr 15];39(6):827-844.e10. Available from: <https://pubmed.ncbi.nlm.nih.gov/34129824/>
72. Piché J, van Vliet PP, Pucéat M, Andelfinger G. The expanding phenotypes of cohesinopathies: one ring to rule them all! <https://doi.org/10.1080/1538410120191658476> [Internet]. 2019 Nov 2 [cited 2022 Apr 15];18(21):2828–48. Available from: <https://www.tandfonline.com/doi/abs/10.1080/15384101.2019.1658476>
73. Kline AD, Moss JF, Selicorni A, Bisgaard AM, Deardorff MA, Gillett PM, et al. Diagnosis and management of Cornelia de Lange syndrome: first international consensus statement. *Nat Rev Genet* [Internet]. 2018 Oct 1 [cited 2022 Apr 15];19(10):649–66. Available from: <https://pubmed.ncbi.nlm.nih.gov/29995837/>
74. Ansari M, Poke G, Ferry Q, Williamson K, Aldridge R, Meynert AM, et al. Genetic heterogeneity in Cornelia de Lange syndrome (CdLS) and CdLS-like phenotypes with observed and predicted levels of mosaicism. *J Med Genet* [Internet]. 2014 [cited 2022 Apr 15];51(10):659–68. Available from: <https://pubmed.ncbi.nlm.nih.gov/25125236/>
75. Boyle MI, Jespersgaard C, Brøndum-Nielsen K, Bisgaard AM, Tümer Z. Cornelia de Lange syndrome. *Clin Genet* [Internet]. 2015 Jul 1 [cited 2022 Apr 15];88(1):1–12. Available from: <https://pubmed.ncbi.nlm.nih.gov/25209348/>
76. Deardorff MA, Noon SE, Krantz ID. Cornelia de Lange Syndrome. *日本小児放射線学会* [Internet]. 2020 Oct 15 [cited 2022 Apr 15];18(1):35–9. Available from: <https://www.ncbi.nlm.nih.gov/books/NBK1104/>
77. Pisani FM. Spotlight on Warsaw Breakage Syndrome. *Appl Clin Genet* [Internet]. 2019 [cited 2022 Apr 15];12:239–48. Available from: <https://pubmed.ncbi.nlm.nih.gov/31824187/>
78. Salari B, Dehner LP. Pseudo-Roberts Syndrome: An Entity or Not? *Fetal Pediatr Pathol* [Internet]. 2020 [cited 2022 Apr 15]; Available from: <https://pubmed.ncbi.nlm.nih.gov/33026893/>
79. Antony J, Vin Chin C, Horsfield JA. Molecular Sciences Cohesin Mutations in Cancer: Emerging Therapeutic Targets. 2021; Available from: <https://doi.org/10.3390/ijms>
80. Antony J, Vin Chin C, Horsfield JA. Molecular Sciences Cohesin Mutations in Cancer: Emerging Therapeutic Targets. 2021; Available from: <https://doi.org/10.3390/ijms>